Experimental evaluation of the use of fins and metal wool as heat transfer enhancement techniques in a latent heat thermal energy storage system

Jaume Gasia[1], José Miguel Maldonado[1], Francesco Galati[2], Marilena De Simone[2], Luisa F. Cabeza[1,*]

[1] GREiA Research Group, INSPIRES Research Centre, University of Lleida, Pere de Cabrera s/n, 25001, Lleida, Spain

[2] Department of Mechanical, Energy and Management Engineering, University of Calabria, P. Bucci 46/C, 87036, Rende, Italy

* Correspondence: lcabeza@diei.udl.cat

Received: date; Accepted: date; Published: date

Abstract: This paper experimentally studies and compares the addition of fins and the addition of metal wool in a latent heat thermal energy storage (TES) system as heat transfer enhancement techniques. Despite the well-known suitability of fins as enhancement technique, their implementation cost in the TES system is one of its main drawbacks. Therefore, the objective of this study is to evaluate the potential of adding a cheap and commercially available metallic wool in order to overcome the abovementioned drawback. In particular, four different latent heat TES systems based on the shell-and-tube heat exchanger concept were designed using n-octadecane as phase change material (PCM). One of them was used as a reference, while in the remaining configurations the heat transfer surface was increased by means of seventeen rectangular fins and by means of metallic wool arbitrarily distributed within the PCM and compacted in a finned shape. Charging and discharging processes with constant heat transfer fluid temperature and flow rate were evaluated from the temperature and heat transfer points of view. Results were focused on the metal wool because is a cheap and handmade solution which can be implemented in an already made heat exchanger. The addition of metal wool showed an enhancement, during the charge, higher than 10% when it was arbitrarily distributed, while compacting the metal wool in a finned shape showed practically no improvement. During the discharge, both metal wool configurations allowed minimal improvements.

Keywords: Thermal energy storage (TES); Phase change material (PCM); Enhancement; Metal wool; Fins; Heat exchanger

Nomenclature

C_p	Specific heat, J/kg·ºC
P	Heat transfer rate, W
R	Function which depends on the measured parameters
t	Time, s
T	Temperature, ºC
w	Uncertainties which are associated to the independent parameters
W	Estimated uncertainty in the final result, value-dependent
x	Independent measured parameters

Greek symbols

ρ	Density, kg/m^3

Subscripts

in	Inlet
out	Outlet

Abbreviations

HEX_NF	Reference heat exchanger
HEX_17F	Heat exchanger with seventeen fins
HEX_MW1	Heat exchanger with the metallic wool placed in a shape similar to a rectangular fin around the HTF tubes bundle
HEX_MW2	Heat exchanger with the metallic wool arbitrarily placed around the HTF tubes bundle
HTF	Heat transfer fluid
PCM	Phase change material
TES	Thermal energy storage

1. Introduction

Thermal energy storage (TES) plays an important role in optimizing thermal processes, helping to reduce the mismatch between the energy demand and supply, taking advantage of waste heat that otherwise would be lost, giving the opportunity to implement peak load shifting strategies, and allowing a better integration of renewable energies. Among the different methods of TES, latent heat TES by means of phase change materials (PCMs) is an attractive option because of its higher energy storage density compared to the sensible heat TES, and the nearly isothermal solidification/melting processes at the PCM phase change transition temperature. However, current cost-effective PCMs have low thermal conductivity (fatty acids: ~0.15 W/m·K; paraffin: ~0.20 W/m·K; salts: ~0.6 W/m·K) [1], which limits the heat transfer during both the charging and discharging processes. The periods of charge and discharge are consequently slowed down and they might cause the thermal process not to be optimized.

Different heat transfer enhancement techniques were studied during the last decades with the aim of increasing the heat transfer rates in TES systems [2-4]. Researchers divided these heat transfer enhancement techniques into two main groups: techniques focused on enhancing the heat transfer between the HTF and the PCM, mainly increasing their heat transfer surface, and techniques focusing on enhancing the heat transfer within the PCM as a result of combining it with highly conductive materials. In the current paper the authors focus on both groups, by studying the addition of fins and the addition of metal wool in a latent heat TES system.

The addition of fins in PCM systems is a heat transfer enhancement technique deeply studied by several researchers [5-11]. It provides high heat transfer rates, as a result of the increase of the heat transfer surface, and therefore, the thermal resistance as well as the charging and discharging processes periods are reduced. The research done regarding this technique was mainly focused on numerically quantifying the influence of the geometrical parameters (number of fins, dimension of the fin, thickness of the fin, and space between fins) and the fins material to the charging and discharging processes. The research conducted regarding the influence of the number of fins and their dimension [5-8] reflected that by increasing these parameters, the heat transfer surface and therefore the heat transfer rates are increased, especially at the initial stages of the process, which causes a reduction of the process periods. As the process continues, the influence of the fins is reduced due to the PCM thermal resistance. On the contrary, the increase of these parameters also leads to a reduction of the volume occupied by the PCM, which reduces the heat capacity of the TES system and influences on the reduction of the process periods.

Hence, if an optimized system is required, these parameters should not exceed a critical value [9]. Lacroix and Benmadda [8] numerically determined that it is more efficient having a few number of longer fins than a large number of shorter fins. The variation of the space between fins is related to the variation of the number of fins, since a higher number of fins means a smaller space between them since the TES system volume is kept constant. The influence of the fins thickness is mainly reflected on the process time and has practically no influence on the heat transfer rates [6,10]. The reason lies on the fact that increasing this parameter results into a decrease of the volume occupied by the PCM while the heat transfer surface is practically kept constant. A numerical study showed that the surfaces of thicker fins showed more uniform temperature than thinner fins, which homogenises the heat transfer rates along the heat transfer surface. Hence, if a balance between the heat transfer rate and the storage capacity is desired, an optimization of this parameter should be performed according to the TES system [6]. Finally, the material of the fins was studied by Laing et al. [11]. They compared four different materials (graphite: k=150 W/m·K; aluminium: k=200 W/m·K; stainless steel: k=20 W/m·K; and carbon steel: k=30 W/m·K). They observed that higher thermal conductivity fins material increased the heat transfer rate and reduced the phase change process times, since the heat transfer surface reached faster a temperature closer to the HTF one. However, other properties such as cost and corrosion should be also studied before selecting the material of the fin.

From the literature review, it is observed that the addition of fins is a suitable solution as a heat transfer enhancement technique. However, two additional drawbacks besides the reduction of the PCM volume are detected. On one hand, the economic cost of the implementation of this technique. On the other hand, the addition of fins is a technique which has to be implemented during the design process of the TES system. The motivation of finding a heat transfer enhancement technique which can overcome these two disadvantages originated the study presented in this paper. The objective of this work is to experimentally evaluate the potential of an economic and easy-to-implement heat transfer enhancement technique, the use of a metallic wool, in a latent heat TES system in terms of heat transfer rates, storage capacity, and cost. Few research was found similar to this concept. Stritih [12] tested an aluminium wool model which showed a 10% performance improvement. That upgrade was attributed to the aluminium side walls which hold the wool, that they worked as fins. Bentilla et al. [13] studied the use of aluminium wool to enhance the PCM effective thermal conductivity and compare it with other metallic fillers such as aluminium and copper foams, and aluminium honeycomb. Results from this study showed that the addition of metal wool presented little improvements and a better performance was

obtained with the metallic honeycomb structures since they provided a larger heat transfer surface area, compared to wool and foams. Reyes et al. [14-16] studied the enhancement of three different aluminium foil configurations obtained from waste soft drink cans (stripes, horizontal perforated disks, and vertical perforated foils) in a latent heat TES system using paraffin wax as PCM. Results showed that enhancements up to 31.1% could be obtained by adding 7.5 wt.% aluminium stripes.

Thus, the authors designed four different latent heat TES systems based on the shell-and-tube heat exchanger concept using n-octadecane as PCM to study the above-mentioned heat transfer enhancement techniques (addition of fins and metal wool). Charging and discharging processes with different flow rates were evaluated from the temperature, power and process time points of views. The results are focused on the use of metal wool as heat transfer enhancement. This upgrade is a cheap and handmade solution which can be implemented in an already built heat exchanger.

2. Materials, experimental setup and methodology

2.1. Materials

The PCM selected in this experimentation is n-octadecane (technical grade, 90% purity), supplied by Alfa Aesar, Germany. The main thermophysical properties of this material are shown in Table 1.

Table 1. Thermophysical properties of n-octadecane [17,18].

Properties	Value
Chemical formula	$CH_3(CH_2)_{16}CH_3$
Melting temperature	27.7 ºC
Latent heat	243.5 J/g
Specific heat capacity (solid)	2.14 kJ/kg·K
Specific heat capacity (liquid)	2.66 kJ/kg·K
Density (solid)	865 kg/m^3
Density (liquid)	785 kg/m^3
Thermal conductivity (solid)	0.190 W/m·K
Thermal conductivity (liquid)	0.148 W/m·K

The HTF used in this experimentation is deionized water, a fluid which has almost all of its mineral ions and anions removed to avoid potential corrosion problems on the HTF piping.

However, for the evaluation of the present experimentation, the authors considered the thermophysical properties of water, which are summarized in Table 2.

Table 2. Thermophysical properties of pure water at atmospheric pressure [19].

Properties	**@ 15ºC**	**@ 40 ºC**
Density	999.1 kg/m^3	992.2 kg/m^3
Dynamic viscosity	1.136 ·10^3 N·s/m^2	0.652 ·10^3 N·s/m^2
Thermal conductivity	0.595 W/m·K	0.653 W/m·K
Thermal expansion coefficient	15.073 ·10^5 1/K	38.530 ·10^5 1/K
Specific heat	4.19 kJ/kg·K	4.18 kJ/kg·K

2.2. Experimental setup

The experimentation performed in the present paper was carried out in an experimental facility located at the University of Lleida (Spain), which is designed to characterize and test latent heat TES systems for mid-low temperature applications (< 100 ºC). Figure 1 shows a detailed schematic view of this experimental setup. It is composed of a 20 l cold HTF storage tank, the temperature of which is controlled by two *JP SELECTA FRIGEDOR* 220 W refrigerated cooling coils and a OVAN TH100E 1600 W immersion thermostat; a 20 l hot HTF storage tank, the temperature of which is controlled by a *JP SELECTA Termotronic* 1600 W immersion thermostat; two three-way valves, which are used to select either the hot or the cold HTF circuit; a *DAB VA 65/180* wet rotor pump, which has a maximum nominal power of 78 W and recirculates the HTF between the HTF storage tanks and the TES system; a *Badger meter Primo Advanced* flow meter, with an accuracy of ±0.25 % of the actual flow; a pin valve, which is used to adjust the HTF flow rate; a data acquisition system, consisting of a *STEP DL-01* data logger and personal computer, with a recording interval of 10 s; and the latent heat TES system. The connections between components are done with 0.5" copper HTF pipes, which are insulated with 18x0.9 mm polyurethane tubes.

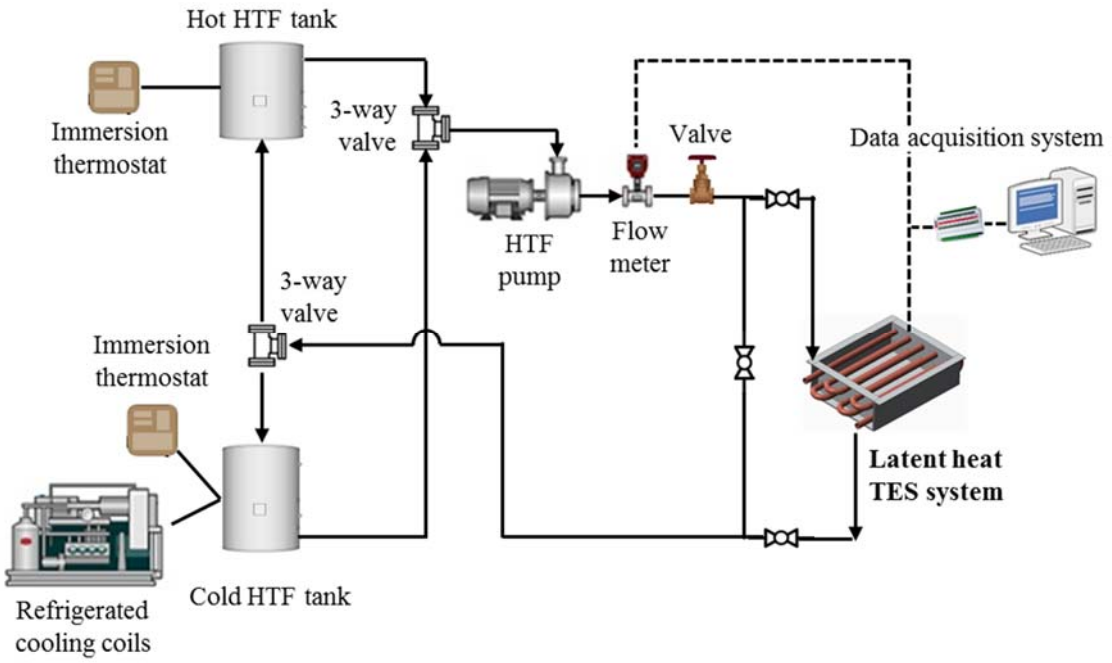

Figure 1. Schematic view of the experimental setup used to perform the experimentation.

Four different latent heat TES systems, based on the shell-and-tube heat exchanger concept, were used in the experimentation presented in this paper (Figure 2). The first TES system was used as a reference (HEX_NF: Figure 2a), while in the remaining configurations their heat exchange surface was increased. In one of them, the heat exchange surface was increased by using rectangular fins (HEX_17F: Figure 2b), and in the other two, a metallic wool placed around the HTF tubes (Figure 2c and Figure 2d). The metallic wool, also known as wire wool, wire sponge, or iron wool, is a bundle of very fine (0.03 mm thick) and flexible sharp-edged steel filaments that is commonly used for industrial and household purposes. The difference between these last two TES systems is that in the first one the metallic wool is placed in a shape similar to a rectangular fin around the HTF tubes bundle (HEX_MW1: Figure 2c), while in the second one the metal wool is arbitrarily placed around the HTF tubes bundle (HEX_MW2: Figure 2d). In the three enhanced latent heat TES systems the objective was to maintain the same quantity of PCM than in the first one. Table 3 summarizes the main characteristics of the four latent heat TES systems.

The temperature of the PCM placed inside the heat exchangers is measured with seven *TMQSS-IM050U* T-type thermocouples, which have an accuracy of ± 0.1 ºC. These temperature sensors are located as shown in Figure 4, at a distance of 40 mm from the bottom of the heat exchanger. Moreover, two additional Pt-100 1/5 DIN class B temperature sensors with an accuracy of ± 0.3 ºC and located at the inlet and outlet of the heat exchangers HTF tubes are used to measure the HTF inlet and outlet temperature.

181 Finally, the latent heat TES systems were insulated with polystyrene in order to reduce
182 the heat losses to the environment. The bottom and lateral walls were insulated with a layer
183 of 80 mm, while the top of the TES systems was insulated with a layer of 20 mm (Figure 3).

184 *2.3. Methodology*

185 The present experimentation consisted of performing in each TES system different
186 charging and discharging processes at a constant flow rate of 0.05 ± 0.002 kg/s. During the
187 charge, the HTF inlet temperature was set at 45 ± 1 ºC and it was considered to be finished
188 when the outlet HTF temperature reached the same temperature than the inlet HTF
189 temperature. Since the setup has a specific circuit for both the hot and cold HTF, there was
190 no homogenization period between processes, and the discharge started immediately after
191 the end of the charge. During the discharge, the HTF inlet temperature was set at 15 ± 1
192 ºC and it was considered to be finished when a steady-state behaviour of the PCM was
193 observed.
194

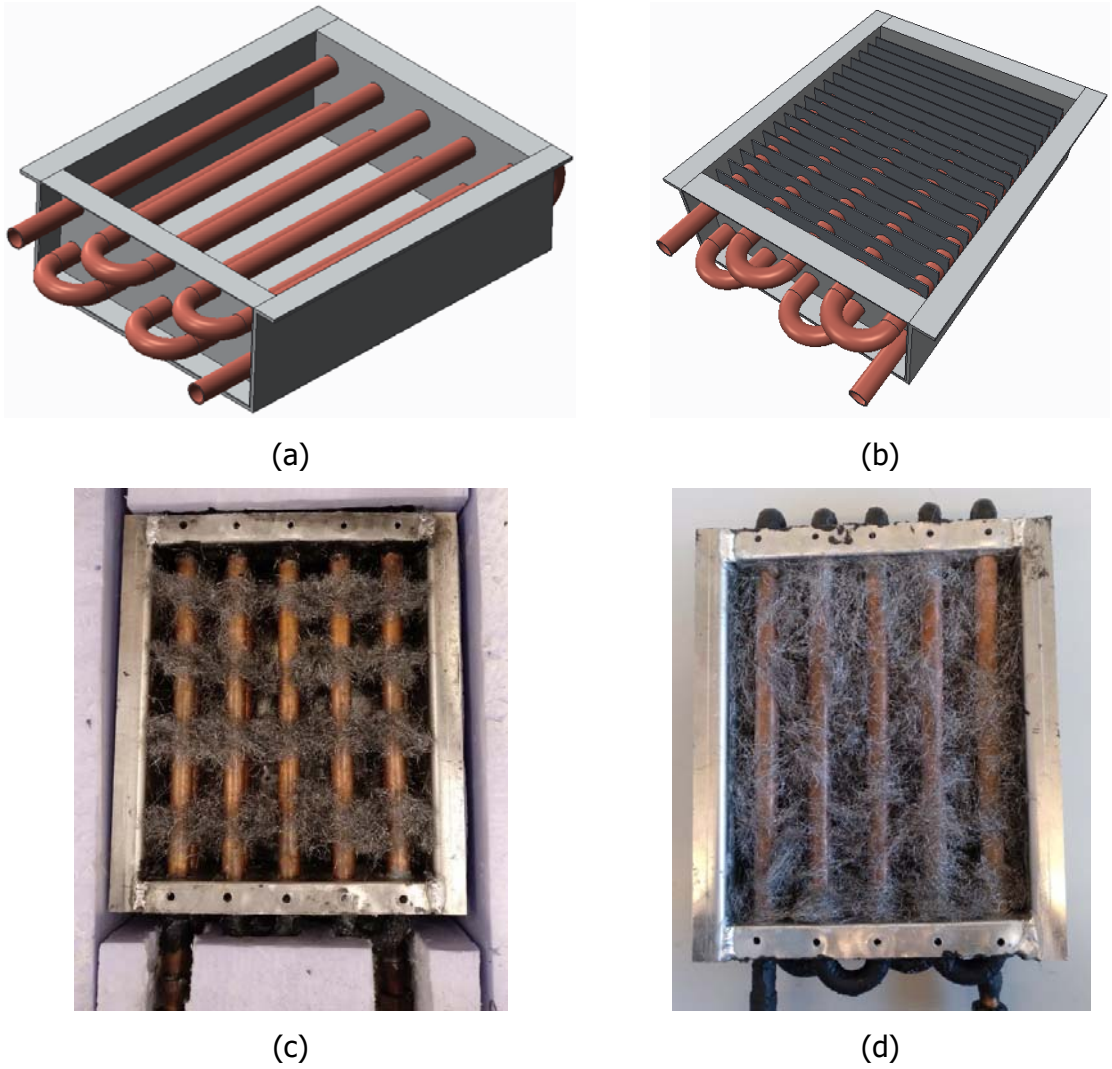

Figure 2. Schematic overview and actual pictures of the different latent heat exchangers tested in the present study: (a) HEX_NF: Reference; (b) HEX_17F: With seventeen fins; (c) HEX_MW1: With metallic wool distributed in a finned shape around the HTF tubes bundle; (d) HEX_MW2: With metallic wool arbitrarily distributed around the HTF tubes bundle.

200

201 Figure 3. Overview of the insulation used in the latent heat TES systems in the present

202 experimentation.

203

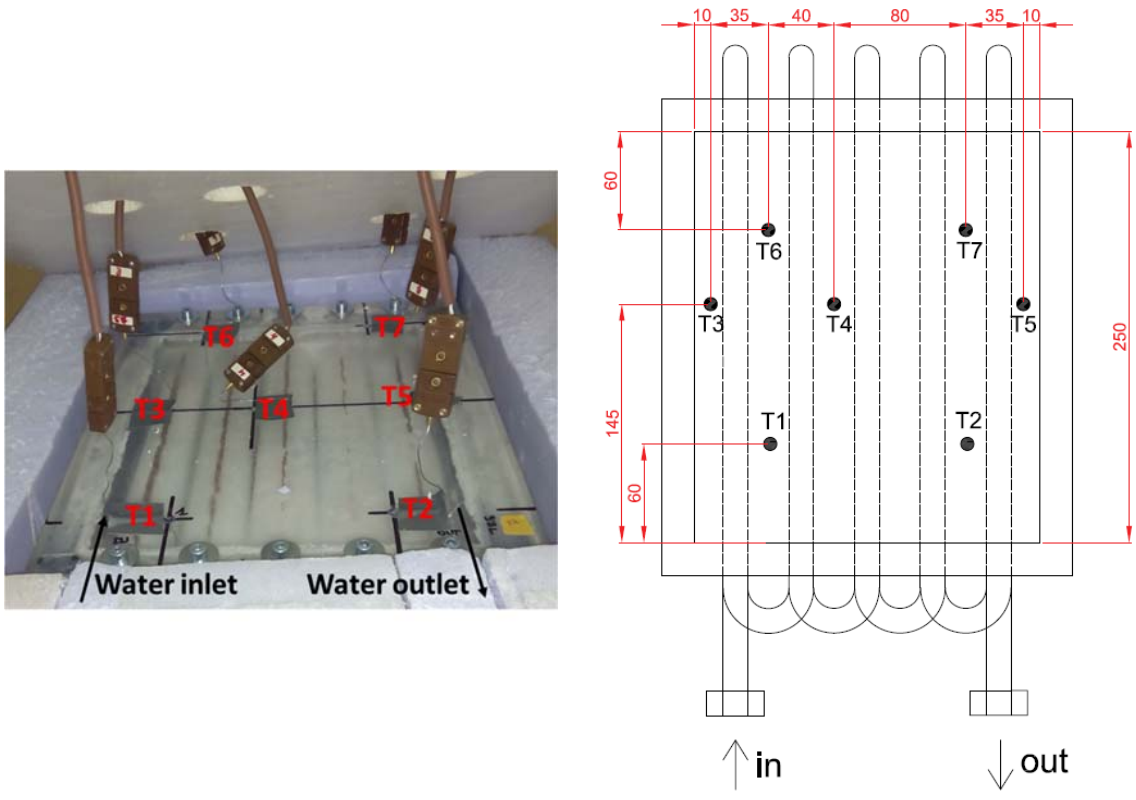

(a) (b)

204 Figure 4. PCM temperature sensors location: (a) Actual location; (b) Schematic view (dimensions in

205 mm).

206 Table 3. Characteristics of the latent heat TES systems analysed and presented in this paper

	HEX_NF	**HEX_17F**	**HEX_MW1**	**HEX_MW2**
Dimensions (length x depth x width)	250 x 85 x 210 mm	250 x 85 x 210 mm	250 x 85 x 210 mm	250 x 85 x 210 mm
Shell material	1050 aluminium alloy	1050 aluminium alloy	1050 aluminium alloy	1050 aluminium alloy
Pipe material	Copper	Copper	Copper	Copper
Type of extended heat exchange surface	None	Fins	Metallic wool	Metallic wool
Material of extended heat exchange surface	-	1050 aluminium alloy	Low-grade carbon steel	Low-grade carbon steel
Heat transfer surface	250 x 85 x 210 mm	Units: 17 Depth: 80 mm Width: 200 mm Thickness: 1 mm Distance between fins: 14 mm	Quantity: 73.8 g Grade: 1 Distribution: Compacted in a finned shape	Quantity: 75.4 g Grade: 1 Distribution: Arbitrary
PCM mass	2666.4 ± 1.4 g	2483.6 ± 0.2 g	2478.2 ± 0.5 g	2482.0 ± 0.2 g

207

3. Results and discussion

3.1. Repeatibility

In the present study each test was repeated minimum three times under the same operating and boundary conditions to ensure repeatability of results. Figure 5 and Figure 6 show different temperature and flow rate profiles during the charging and the discharging processes. Specifically, Figure 5 shows the mean inlet HTF temperature and flow rates, as well as their standard deviations during both charging and discharging processes of the four latent heat TES systems. Notice that in both charging and discharging processes very similar trends are observed. The maximum standard deviation in temperature is 1.5 ºC over 43.7 ºC during the charge. However, this deviation drops to values lower than 1 ºC after 20 min, once the temperature stabilization process of the immersion thermostat reaches the steady state. During the discharge, a maximum standard deviation in temperature of 8.4 ºC over 41.6 ºC is observed. Nevertheless, this deviation rapidly decreases to values lower than 1ºC after 7 minutes, for analogous reason. Moreover, Figure 5 also shows that the flow rate is more stable than the temperature. During the charging process, the maximum standard deviation is 0.12 L/min over 1.47 L/min, while the mean deviation during the first 30 minutes is 0.09 L/min. On the other hand, the discharging process presents a similar mean deviation during the first 30 min (0.08 L/min), despite showing values of 0.2 L/min over 1.6 L/min as maximum deviation.

Figure 6 presents the three experiments which were carried out on the latent heat TES system with the metal wool compacted in a finned shape (HEX_MW1). It shows the temperature profiles of the PCM at two different locations (evaluated by the temperature sensors T1 and T2) as well as the inlet HTF temperature evolution during the discharging process. In this case, it can be seen that the variation among the three experiments is negligible. The maximum standard deviation is 0.86 ºC over 42.7 ºC but after 15 min is no longer higher than 0.15 ºC. Moreover, the HTF inlet temperature shows a maximum deviation of 3.7 ºC over 44.5 ºC, however, after 5 min this value is kept below 0.5 ºC. Both deviations can be related with the uncertainty of the temperature sensors.

Similar results were obtained on the others latent heat TES configurations. Hence, results from the repeatability tests show that the methodology adopted for the present experimentation produced repeatable values.

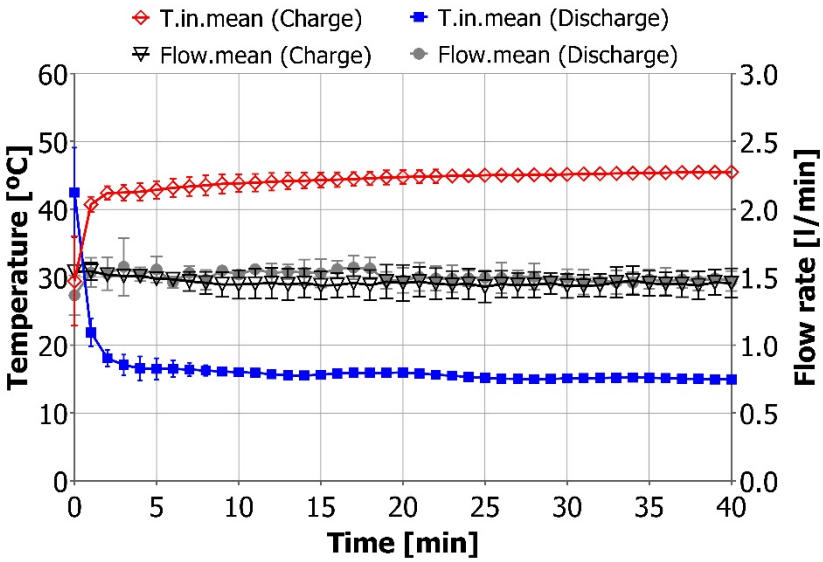

Figure 5. HTF inlet temperature and flow rate profiles for the four case studies evaluated in this paper.

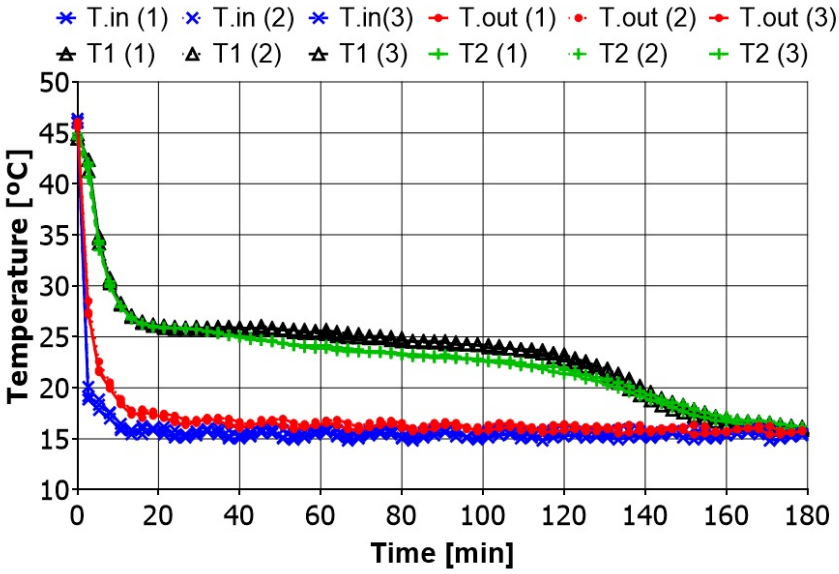

Figure 6. Repeatability tests for the case study of the latent heat TES system with the metal wool compacted in a finned shape (HEX_MW1): HTF and PCM temperature profiles during the discharging process.

3.2. Charging process

Hereunder, the results obtained during the charging process in all latent heat TES systems evaluated in the present study can be found. Figure 7 shows the HTF and PCM temperature evolution during the charge in the reference latent heat TES system (HEX_NF). This difference in time is mainly due to the sensor position inside the TES system (Figure 4), as previously mentioned. It is also produced because of the sensor displacement as a

result of the PCM density variation during the phase change, which causes the sensor to be pushed towards the HTF piping (i.e. T4 and T5).

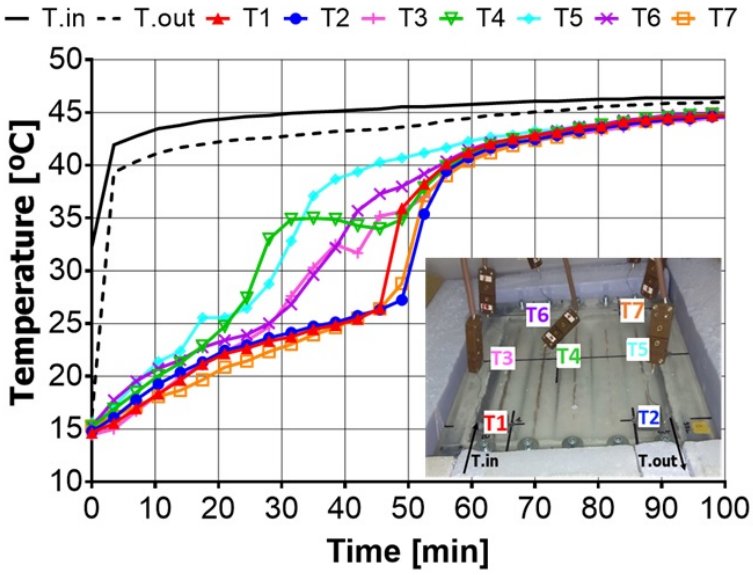

Figure 7. PCM and HTF temperature profiles in the reference latent heat TES system (HEX_NF) during the charging process.

In order to make the comparison of results more understandable for the reader, in the following charts only four out of the seven monitored PCM temperatures will be shown (T1, T2, T6 and T7). T1 and T2 sensors were chosen because of their location close to the HTF inlet and outlet, respectively, while T6 and T7 were chosen because of their opposite location to the latter mentioned.

Figure 8 shows the comparison of the temperature profiles of the four different heat exchanger configurations during the charging process. It can be observed that the heat exchanger which shows a faster charge is the one with fins (HEX_17F). The reason lies on the increase of the heat transfer surface combined with the higher thermal conductivity of aluminium. This allows the heat transfer surface to achieve faster a temperature close to the HTF one and therefore, allowing a higher quantity of PCM to be in contact with a high temperature surface. On the other hand, both latent heat TES systems which have metal wool (HEX_MW1 and HEX_MW2) enhance the heat transfer and present an improvement in terms of time if compared to the reference TES system (HEX_NF). In particular, the TES system with the metal wool arbitrarily distributed within the PCM (HEX_MW2) shows a better behaviour than the TES system with the metal wool compacted in finned shape (HEX_MW1,) since it needs less time to finish the charging process. The end of the charging process can

278 be considered when the PCM temperature is equal to the heat transfer temperature ± 0.3
279 ºC.

280

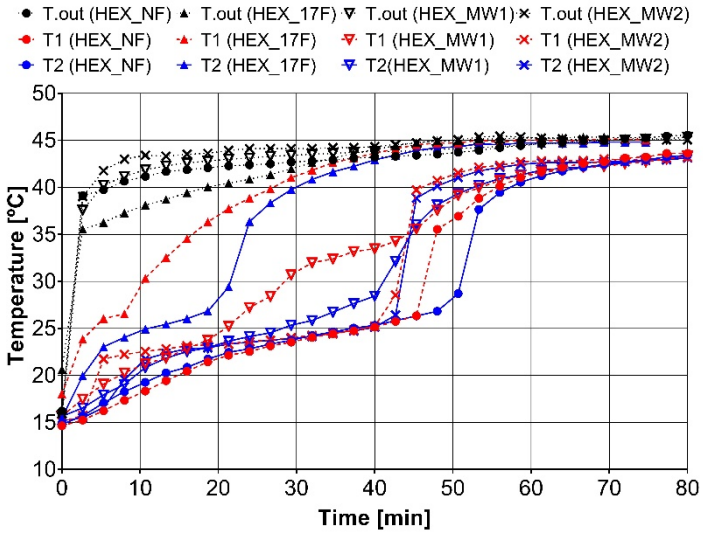

(a)

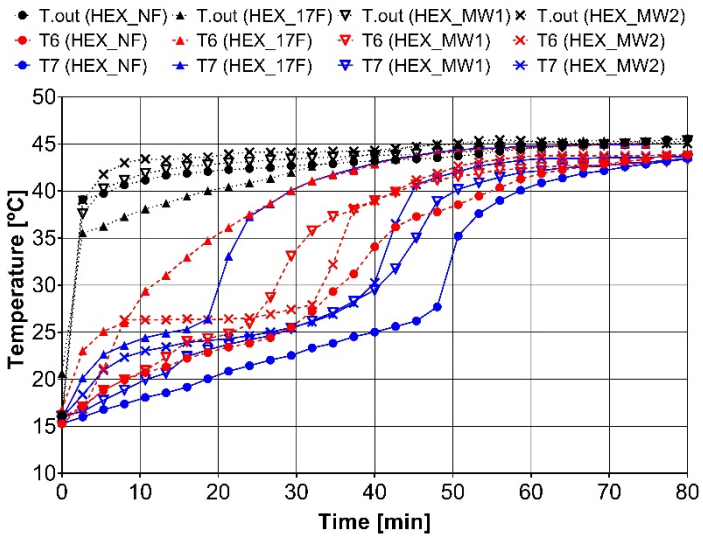

(b)

281 Figure 8. PCM and HTF temperature comparison among the four different latent heat TES systems
282 during the charging process: (a) The PCM temperature sensors are T1 and T2; (b) The PCM
283 temperature sensors are T6 and T7.

284 Figure 9 and the Table 4 show the comparison of the heat transfer during the charging
285 process in the four different latent heat TES systems. Similarly to what it is observed in the
286 temperature profiles, the finned heat exchanger (HEX_17F) is the system that shows better
287 results. The difference between the finned and the metal wool TES systems lies on the
288 conduction heat transfer mechanism. The fins are bonded to the HTF pipes, unlike the metal
289 wool which is just in contact with the piping. Moreover, the fins have a continuous surface,

290 which allows the heat to be transferred without discontinuities. On the other hand, the metal
291 wool is made of several wires, which do not create a continuous surface, not even when it
292 is compacted in a finned shape. Finally, it has to be taken into account that the heat
293 transferred from the HTF to the metal wires is rapidly released to the PCM because of the
294 high convection coefficient within the wire. Therefore, the heat transfer to the wire through
295 conduction cannot match the heat release rate by convection. Additionally, the material of
296 the fins (aluminium) is around four times better in terms of thermal conductivity than the
297 material of the metal wool (low grade carbon steel). All these characteristics cause the TES
298 system with fins to have the highest heat transfer rate.

299 It is also observed that the two TES systems with metal wool as heat transfer
300 enhancement technique show better results than the reference system. In particular, the
301 TES system with the metal wool arbitrarily distributed (HEX_MW2) has a better performance
302 than the TES system with the metal wool compacted in a finned shape (HEX_MW1). This
303 difference is mainly due to the fact that the arbitrary distribution allows more metal wires
304 to be in contact with the PCM, while the finned shape distribution causes some metal wires
305 to be in contact with themselves but not with the PCM. Therefore, for the same quantity of
306 metal wool, lower heat transfer surface is achieved. As it can be seen in Table 4, by randomly
307 distributing the metal wool in the TES system (HEX_MW2), the heat transfer can be
308 improved more than 10% during the first 30 min if compared to the reference case
309 (HEX_NF), while compacting the metal wool in a finned shape (HEX_MW1) allows minimal
310 improvements.

311

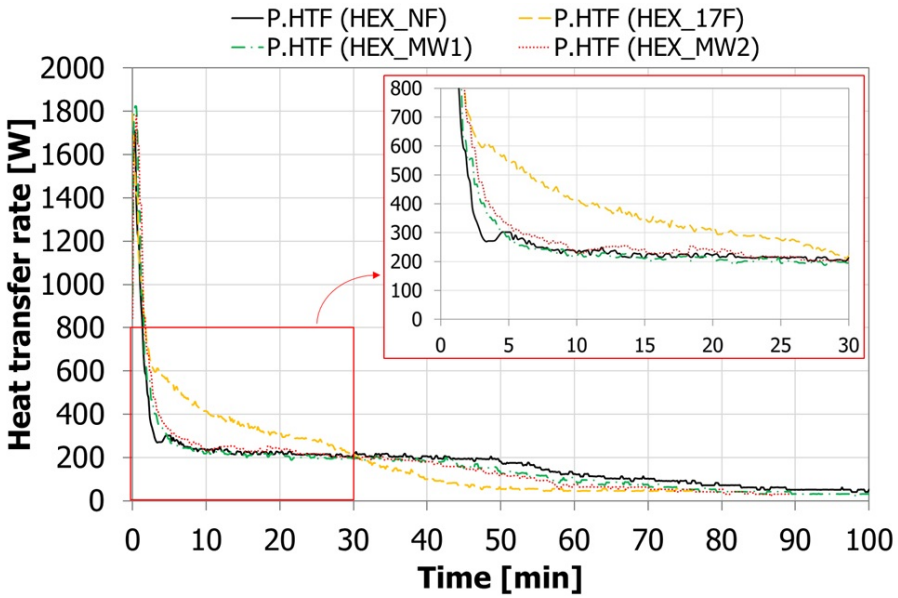

312

313 Figure 9. Heat transfer rate comparison between the four different latent heat TES systems during
314 the charging process.

Table 4. Heat transfer rate comparison between the four different latent heat TES systems during the charging process and their difference compared to the reference system (HEX_NF).

Time	HEX_NF	HEX_17F		HEX_MW1		HEX_MW2	
[min]	[W]	[W]	[%]	[W]	[%]	[W]	[%]
5	631.51	837.50	32.6%	713.63	13.0%	775.89	22.9%
10	445.82	657.53	47.5%	481.52	8.0%	530.55	19.0%
15	374.49	565.69	51.1%	395.50	5.6%	436.23	16.5%
20	336.69	506.28	50.4%	350.43	4.1%	386.42	14.8%
25	312.83	463.33	48.1%	321.09	2.6%	354.11	13.2%
30	295.75	427.53	44.6%	300.60	1.6%	329.87	11.5%
60	240.53	261.30	8.6%	229.14	-4.7%	238.10	-1.0%

3.2. Discharging process

Hereunder, the results obtained during the PCM solidification process for all TES systems are shown. Figure 10 shows the HTF and PCM temperature evolution during the discharge in the reference latent heat TES system (HEX_NF). Unlike the charging process, all temperature sensors show a similar behaviour, being the slight differences due to sensitive changes in the thermocouple position because of the phase change layer. It can also be observed that the discharging process takes longer than the charging one (200 min instead of 80 min for charging). The reason lies in the fact that the temperature difference between the inlet and phase change inlet temperature when charging is higher than the difference between the phase change and the discharging inlet temperature. Also it has to be pointed out that the melting process is mainly governed by convection whilst conduction is the dominant heat transfer mechanism during solidification; and the PCM thermal resistance through conduction is very high.

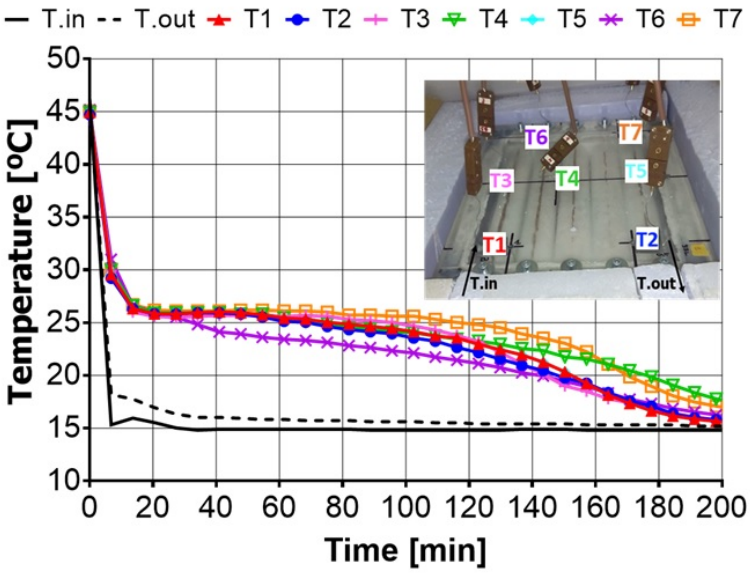

Figure 10. PCM and HTF temperature profiles in the reference latent heat TES system (HEX_NF) during the discharging process.

Figure 11 shows the comparison between the four different TES systems, in terms of temperature. This figure shows the outlet temperature of the HTF and the PCM temperatures from the T1, T2, T6, and T7 sensors point of view. Notice that the best solution, identically to the charging process, is the finned system (HEX_17F). The main reason, as previously said, is the better thermal conductivity performance of aluminium in couple with a larger heat transfer surface provided by the fins. Hence, the discussion is focused on the enhancement of innovative and cheap proposal presented in this paper: the use of commercial metal wool. It is observed that both systems using metal wool present little improvement compared to the reference system, since they reach earlier the steady state. On the other hand, worse results are observed in the heat transfer profiles (Figure 12 and Table 5), which do not match with the results observed in the temperature profiles. This is due to the temperature stabilization process that took place in the HTF cold tank during the first minutes of discharge. Thus, as conduction is the main heat transfer mechanism, and taking into account the error due to the temperature measurement, it can be concluded that metal wool as heat transfer enhancement technique has no effect on the heat exchanger performance during the discharging process. The improvement due to the steel-wire high convection coefficient is soon neglected when the PCM is solidified around the wire.

It is clear that modifications should be applied to the metal wool in order to improve its performance. One of the solutions should be the modification of the material so as to use one with higher thermal conductivity, but then the cost might increase (due to the cost of

355 the material but mostly to the mass production possible in this metal wool). The second
356 solution should be the modification of the geometry. If this parameter is changed by
357 increasing the diameter of the metal wires, the heat transfer would increase. However, both
358 solutions should follow the same ideology than the initial technique to be a feasible solution:
359 cheap, homemade and accessible.

360

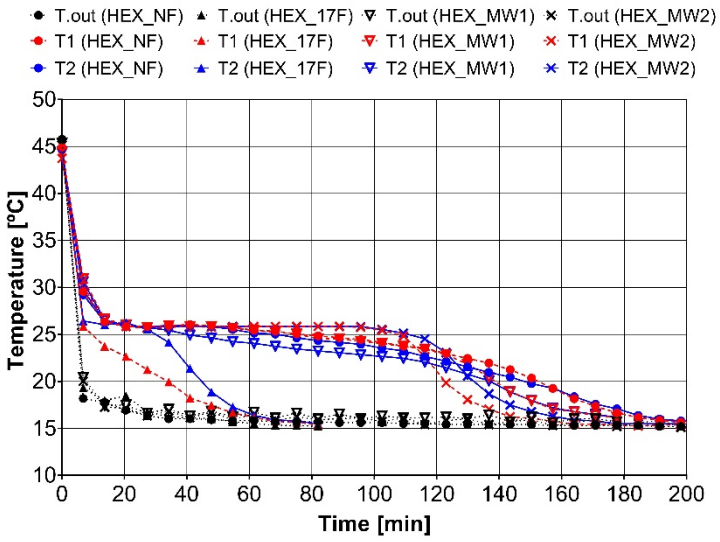

(a)

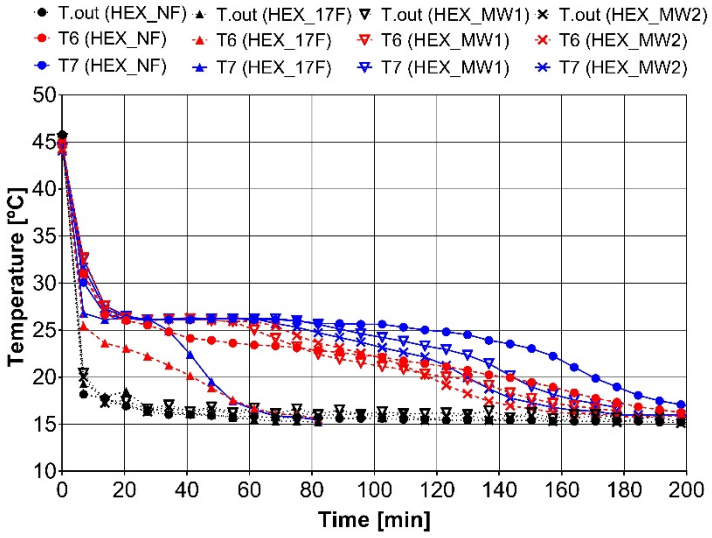

(b)

361 Figure 11. PCM and HTF temperature comparison among the four different latent heat TES systems
362 during the discharging process: (a) The PCM temperature sensors are T1 and T2; (b) The PCM
363 temperature sensors are T6 and T7.

364

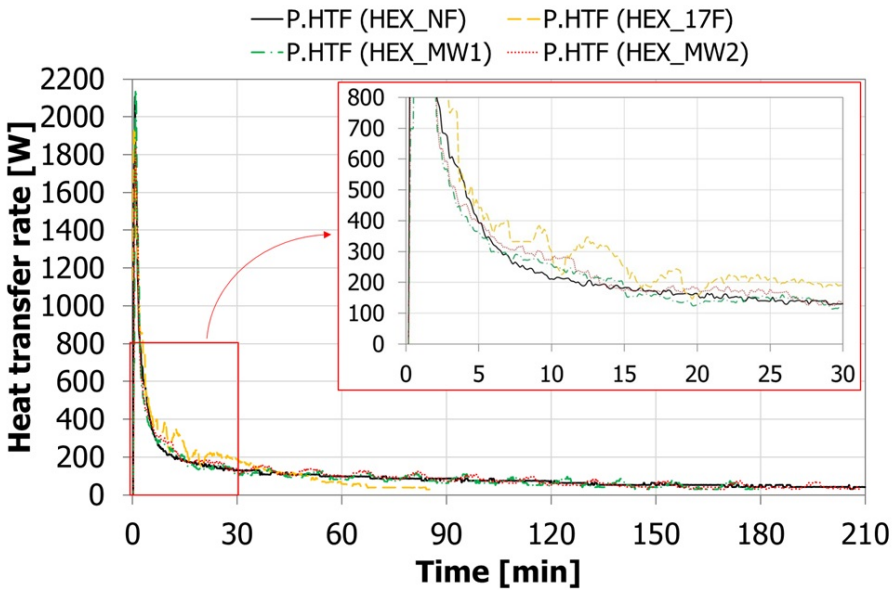

Figure 12. Heat transfer rate comparison between the four different latent heat TES systems during the discharging process.

Table 5. Heat transfer rate comparison between the four different latent heat TES systems during the discharging process and their difference compared to the reference system (HEX_NF).

Time	HEX_NF	HEX_17F		HEX_MW1		HEX_MW2	
[min]	[W]	[W]	[%]	[W]	[%]	[W]	[%]
5	831.49	984.00	18.3%	769.71	-7.4%	776.07	-6.7%
10	557.69	678.68	21.7%	532.98	-4.4%	549.51	-1.5%
15	438.80	551.83	25.8%	430.27	-1.9%	443.45	1.1%
20	372.00	465.42	25.1%	360.29	-3.1%	377.04	1.4%
25	327.88	414.26	26.3%	317.30	-3.2%	336.49	2.6%
30	296.25	378.39	27.7%	287.91	-2.8%	304.62	2.8%
60	204.37	245.99	20.4%	198.80	-2.7%	214.45	4.9%

3.4. Uncertainties analysis

In order to show the impact on the results of the different parameter uncertainties, an uncertainty analysis was performed. This analysis is required to determine and validate the present study. The uncertainties of the measured parameters are shown in Table 6, while the specific heat and the density of the HTF were calculated from the correlations presented in Eq.1 and Eq. 2 [20]:

$$\rho_{HTF} = 1.38e^{-5} \cdot T_{HTF}^2 - 5.63e^{-3} \cdot T_{HTF}^2 + 3.6e^{-3} \cdot T_{HTF} + 1000 \quad (1)$$

$$Cp_{HTF} = 2.69e^{-9} \cdot T_{HTF}^4 - 6.63e^{-7} \cdot T_{HTF}^3 + 6.67e^{-5} \cdot T_{HTF}^2 - 2.67e^{-3} \cdot T_{HTF} + 4.21 \quad (2)$$

Table 6. Uncertainties of the different parameters involved in the analyses of the present study.

Parameter	Units	Sensor	Accuracy
Temperature	ºC	Pt-100 1/5 DIN class B	± 0.3
Temperature	ºC	TMQSS-IM050U T-type thermocouples	± 0.1
Flow rate	L/min	Badger meter Primo Advanced	± 0.25%

Eq. 3 allows estimating the uncertainties of the HTF properties as well as of the HTF heat transfer rates. The uncertainty was estimated for every single time step monitored, so the mean value is used. Table 7 shows the average uncertainty in HTF thermophysical properties and power of the different processes carried out.

$$W_R = \left[\left(\frac{\partial R}{\partial x_1}\cdot w_{x_1}\right)^2 + \left(\frac{\partial R}{\partial x_2}\cdot w_{x_2}\right)^2 + \cdots + \left(\frac{\partial R}{\partial x_n}\cdot w_{x_n}\right)^2\right]^{1/2} \quad (3)$$

being W_R the estimated uncertainty in the final result, R the function which depends on the measured parameters, x_n are the different independent measured parameters, and w_x are the uncertainties associated to those independent parameters.

Table 7. Estimated uncertainties of the HTF thermophysical properties and power.

	Heat exchanger design	Uncertainty of the HTF					
		Density		Specific heat		Heat transfer rate	
		[± kg/m³]	[± %]	[± kJ/kg·ºC]	[± %]	[± kW]	[± %]
Charging Process	HEX_NF	0.03	0.003	2.08 E-5	0.0005	0.0120	6.30
	HEX_17F	0.02	0.0018	1.25 E-5	0.0003	0.0073	3.30
	HEX_MW1	0.0284	0.0287	1.53 E-5	0.0004	0.0105	4.55
	HEX_MW2	0.0296	0.0029	1.81 E-5	0.0004	0.0120	5.64
Discharging Process	HEX_NF	0.0091	0.0009	5.37 E-5	0.0013	0.0085	8.81
	HEX_17F	0.0093	0.0009	5.26 E-5	0.0013	0.0086	8.06
	HEX_MW1	0.0102	0.001	5.2 E-5	0.0012	0.0083	7.53
	HEX_MW2	0.0087	0.0008	5.52 E-5	0.0013	0.0086	9.48

4. Conclusions

This paper experimentally investigates the performance of three different heat transfer enhancement techniques in a latent heat TES system: the addition of metallic (aluminium) fins, the addition of metal (low grade carbon steel) wool arbitrarily distributed within the

TES system, and the addition of metal wool compacted in a finned shape. The objective of this paper is to assess the benefits, and more important, the weak points of adding metal wool. Research findings of this study provided evidence that the currently available metal wool cannot compete against the aluminium fins. However, it has to be pointed out that metal wool is a cheap and homemade solution which can improve, when it is arbitrarily distributed within the TES system, the charging process up to 14% in terms of heat transfer if compared to a system without enhancement technique. On the other hand, the addition of metal wool showed little improvement during the discharging process.

Author Contributions: Jaume Gasia, José Miguel Maldonado and Luisa F. Cabeza conceived and designed the study; Jaume Gasia and José Miguel Maldonado built the experimental setup; Jaume Gasia, José Miguel Maldonado and Francesco Galati performed the experiments; all co-authors collaborated on the interpretation of the results and on the preparation of the manuscript.

Acknowledgments: The work was partially funded by the Spanish government (ENE2015-64117-C5-1-R (MINECO/FEDER)). The authors would like to thank the Catalan Government for the quality accreditation given to their research group (2017 SGR 1537). GREA is certified agent TECNIO in the category of technology developers from the Government of Catalonia. Jaume Gasia would like to thank the Departament d'Universitats, Recerca i Societat de la Informació de la Generalitat de Catalunya for his research fellowship (2018 FI_B2 00100). José Miguel Maldonado would like to thank the Spanish Government for his research fellowship (BES-2016-076554). Francesco Galati would like to thank the Erasmus+ Programme: Traineeship Bet for Jobs for his research fellowship

Conflicts of Interest: The authors declare no conflict of interest.

References

1. Cabeza L.F, Castell A, Barreneche C, de Gracia A, Fernández A.I. Materials used as PCM in thermal energy storage in buildings: A review. *Renew Sust Energ Rev* **2011**, *15(3)*, 1675-1695, DOI: 10.1016/j.rser.2010.11.018.
2. Bose P, Amirtham V.A. A review on thermal conductivity enhancement of paraffin wax as latent heat energy storage material. *Renew Sust Energ Rev* **2016**, 65, 81-100, DOI: 10.1016/j.rser.2016.06.071.
3. Fan L, Khodadadi J.M. Thermal conductivity enhancement of phase change materials for thermal energy storage: A review. *Renew Sust EnergRev* **2011**, 15, 24-46, DOI: 10.1016/j.rser.2010.08.007.

4. Agyenim F, Hewitt N, Eames P, Smyth M. A review of materials, heat transfer and phase change problem formulation for latent heat thermal energy storage systems (LHTESS). *Renew Sust EnergRev* **2010**, 14, 615-628, DOI: 10.1016/j.rser.2009.10.015.
5. Seeniraj R, Velraj R, Lakshmi Narasimhan N. Thermal analysis of a finned-tube LHTS module for a solar dynamic power system. *Heat and Mass Transf* **2002**, 38, 409-417, DOI: 10.1007/s002310100268.
6. Hosseinizadeh S, Tan F, Moosania S. Experimental and numerical studies on performance of PCM-based heat sink with different configurations of internal fins. *Appl Therm Eng* **2011**, 31, 3827-3838, DOI: 10.1016/j.applthermaleng.2011.07.031.
7. Tao Y, He Y. Effects of natural convection on latent heat storage performance of salt in a horizontal concentric tube. *Appl Energ* **2015**, 143, 38-46, DOI: 10.1016/j.apenergy.2015.01.008.
8. Lacroix M, Benmadda M. Numerical simulation of natural convection-dominated melting and solidification from a finned vertical wall. *Numer Heat Tr A Appl* **1997**, 31, 71-86, DOI: 10.1080/10407789708914026.
9. Gharebaghi M, Sezai I. Enhancement of heat transfer in latent heat storage modules with internal fins. *Numer Heat Tr A Appl* **2007**, 53, 749-765, DOI: 10.1080/10407780701715786.
10. Guo C, Zhang W. Numerical simulation and parametric study on new type of high temperature latent heat thermal energy storage system. *Energy Convers Manag* **2008**, 49, 919-927, DOI: 10.1016/j.enconman.2007.10.025.
11. Laing D, Bauer T, Steinmann W.D, Lehmann D. Advanced high temperature latent heat storage system – Design and test results. Proceedings of The 11th International Conference on Thermal Energy Storage (Effstock), Stockholm, Sweeden, 2009.
12. Stritih, Uros. An experimental study of enhanced heat transfer in rectangular PCM thermal storage. International Journal of Heat and Mass Transfer **2004**, 47, pp. 2841-2847.
13. Bentilla EW, Sterrett KF, Karre LE. Research and development study on thermal control by use of fusible materials. *Northrop Space Laboratories Interim Report (NSL-65-16-1). NASA Marshall Space Flight Center* **1966**. Available at: http://ntrs.nasa.gov/search.jsp?R=19660017401.
14. Reyes A, Negrete D, Mahn A, Sepúlveda F. Design and evaluation of a heat exchanger that uses paraffin wax and recycled materials as solar energy accumulator. *Energy Convers Manag* **2014**, 88, 391–398, DOI: 10.1016/j.enconman.2014.08.032.
15. Reyes A. Henríquez-Vargas L, Aravena A, Sepúlveda F. Experimental analysis, modeling and simulation of a solar energy accumulator with paraffin wax as PCM. *Energy Convers Manag* **2015**, 105, 189–196. DOI: 10.1016/j.enconman.2015.07.068.
16. Reyes A. Henríquez-Vargas L, Rivera J, Sepúlveda F. Theoretical and experimental study of aluminum foils and paraffin wax mixtures as thermal energy storage material. *Renew Energ* **2017**, 101, 225-235, DOI: 10.1016/j.renene.2016.08.057.
17. Lacroix M. Numerical simulation of a shell-and-tube latent heat thermal energy storage unit. *Sol Energy* **1993**, 50, 357-367, DOI: 10.1016/0038-092X(93)90029-N.

18. Adine H.A, El Qarnia H. Numerical analysis of the thermal behaviour of a shell-and-tube heat storage unit using phase change materials. *Appl Math Model* **2009**, 33, 2132-2144, DOI: 10.1016/j.apm.2008.05.016.
19. Kukulka D.J. Thermodynamic and Transport Properties of Pure and Saline Water, MSc Thesis, State University of New York at Buffalo, USA, 1981.
20. Holman J.P. *Experimental Methods for Engineers*, 8th ed. McGraw-Hill, New York, USA, 2012; ISBN: 0073529303.